

## AlphaLISA Technology

## Author:

Jeanine Hinterneder, PhD

PerkinElmer, Inc.  
Hopkinton, MA

## Evaluating the Effects of Gefitinib and Cetuximab in Two EGFR-Overexpressing Cancer Models Using a Biomarker Detection and Imaging Platform – a Systems Approach

### Introduction

The physiological function of the epidermal growth factor receptor (EGFR) is to regulate epithelial tissue development and homeostasis.

However, its overexpression and activation are strongly linked to oncogenesis and tumor progression

in many types of cancers including lung, breast, colon and those of epidermoid origin.<sup>1-4</sup>

Of the two major EGFR-targeted therapies developed, one class utilizes humanized monoclonal antibodies to target the extracellular ligand-binding domain of the EGFR, thus blocking endogenous ligand binding and receptor activation. The second class of therapeutic drugs are tyrosine kinase inhibitors (TKIs), which are ATP mimetics that bind to the intracellular kinase pocket of the receptor, preventing phosphorylation and further signal transduction. Though both these anti-cancer therapies have proven to be effective, resistance to individual EGFR inhibitors eventually develops, leading to the need for more studies probing the efficacy of combinatorial drug treatments in the clinic.<sup>5-7</sup>

We present here data examining the effects of individual and combined treatment with the FDA-approved drugs cetuximab (Erbix<sup>®</sup>) and gefitinib (Iressa<sup>®</sup>), both targeting the EGFR but via different mechanisms (illustrated in Fig 1A), in two human cancer-derived cell lines. Cetuximab is a humanized monoclonal antibody that binds to the extracellular domain of EGFR, designed to block ligands, such as EGF, from binding to the receptor and activating downstream signaling.<sup>8-9</sup> Gefitinib is a small molecule TKI that blocks EGFR auto-phosphorylation.<sup>10</sup> To characterize the effects of these two EGFR-targeted therapies, AlphaLISA<sup>®</sup> technology and the EnSight<sup>®</sup> multimode plate reader were used to assess the effects of treatment on proliferation and the expression of key tumor biomarkers. These include immune checkpoint proteins and secreted chemokines in cellular models of skin cancer and non-small cell lung carcinoma (NSCLC).

AlphaLISA technology enables rapid detection of molecules of interest in a homogeneous, no-wash format with greater sensitivity and allows for the use of low sample volumes (5  $\mu$ L or less). In the assay schematic illustrated in Figure 1B, a biotinylated anti-EGFR antibody binds to streptavidin-coated Alpha Donor beads while another anti-EGFR antibody is conjugated directly to AlphaLISA Acceptor beads. In the presence of human EGFR, both antibodies bind the analyte and bring the Donor and Acceptor beads into proximity. Excitation of the Donor beads with light at 680 nm provokes the release of singlet oxygen molecules that activate the Acceptor beads resulting in the emission of light detected with a maximum at 615 nm. The emission is proportional to the concentration of EGFR protein in the sample and can be read on a plate reader equipped with Alpha detection, such as the EnSight (Figure 1C). This multimode plate reader is also equipped with a well imaging module that enabled us to assess treatment effects on cellular proliferation measured with image-based cytometry.

## Materials and Methods

### Cell Culture and Treatment

The human epidermoid carcinoma-derived cell line A431 (A-431; ATCC<sup>®</sup> CRL-1555<sup>™</sup>) and human lung cancer derived cell line A549 (A549; ATCC<sup>®</sup>, #CCL-185<sup>™</sup>) were grown in DMEM (ATCC<sup>®</sup>, #30-2002) and F-12K Medium (ATCC<sup>®</sup>, #30-2004) respectively,

supplemented with 10% FBS (ThermoFisher, #11875-093). Cells were seeded at 10,000 A431 cells or 5,000 A549 cells per well (in 100  $\mu$ L of media) into black, 96-well ViewPlates<sup>™</sup> (PerkinElmer, #6005182) and allowed to attach overnight. These initial seeding densities were previously determined to result in cultures becoming no more than 90% confluent after three days without additional treatment (data not shown). Treatment with drugs and EGF was administered the next day and effects measured two days later. To assess the effects of EGF on each cell type, a titration of varying concentrations of recombinant human EGF (rh EGF; R&D Systems, #236-EG-200) were diluted in culture media and added directly to wells at 2X the final concentration resulting in a final well volume of 200  $\mu$ L. To examine the effects of each drug, varying concentrations of the small molecule inhibitor gefitinib (ZD1839; Selleckchem, #S1025) and the EGFR-specific monoclonal antibody cetuximab (Selleckchem, #A2000) were diluted in culture media and added directly to wells. After 30 minutes of exposure to inhibitors, half the wells were then treated with the specified EGF concentration and cultures were incubated for two more days.

### Well Imaging, Cell Counting and Sample Collection

Two days after treatment, supernatant samples were transferred to polypropylene StorPlates<sup>™</sup> (PerkinElmer, #6008290) and frozen at -20  $^{\circ}$ C until further use. Cell nuclei were then labeled by the addition of Hoechst 33342 (Life Technologies, #H3570) at 5  $\mu$ g/mL final concentration in culture media and plates were imaged after 15 minutes on the EnSight multimode plate reader. Automated cellular imaging and counting of Hoechst-labeled cell nuclei were done using the well-imaging module on the EnSight, using brightfield optics and UV filters. Cellular nuclei were automatically identified and counted from the images and total cell number per well determined by the EnSight system's Kaleido<sup>™</sup> software.

Immediately after imaging (less than 30 minutes from Hoechst addition), the remaining media were aspirated and cells were lysed by the addition of 100  $\mu$ L of AlphaLISA Lysis Buffer for 30 minutes at room temperature on a rotational shaker (DELTA<sup>®</sup> PlateShaker set at 600-700 RPM). Lysates were then also transferred to StorPlates and frozen until assessment with AlphaLISA detection assays. Note that the residual Hoechst 33342 stain present in lysate samples does not interfere with the detection assays.

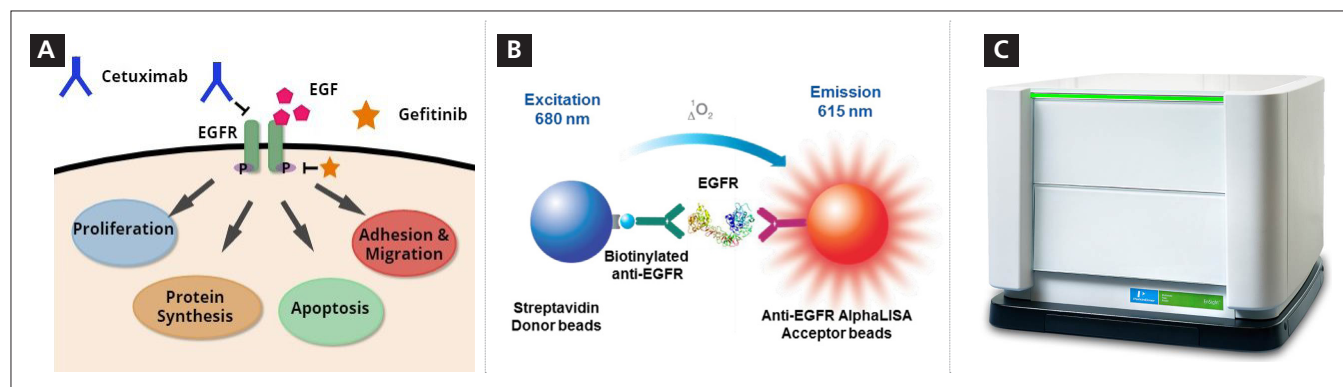


**Figure 1. EGFR signaling and AlphaLISA detection assay models.** A) Model showing the different mechanisms of action of gefitinib and cetuximab on EGFR activation and downstream processes that may be affected by treatment. B) Schematic of an AlphaLISA detection assay for EGFR protein that can be detected using the (C) EnSight multimode plate reader.

## AlphaLISA Detection Assays

For AlphaLISA detection assays, 5  $\mu$ L samples were distributed into separate assay plates (AlphaPlate™-384; PerkinElmer, #6005350) for each biomarker assessed and the assays were performed as indicated in the technical data sheets. Data presented here were generated using PerkinElmer's AlphaLISA assays for the following (human) targets: EGFR (#AL340), PD-L1 (#AL355), CD276 (#AL3060), CXCL1/GRO- $\alpha$  (#AL349), IL-8 (#AL370), VEGF (#AL201), and TIMP-2 (#AL3091). All assays were run on supernatant or lysate samples from the same wells of the original cell culture plates. In addition to the biomarker detection assays, the AlphaLISA EGF/EGFR binding kit (#AL366) was used to verify and illustrate cetuximab inhibition of the ligand binding domain of EGFR. The binding assay was run following the competition assay procedure described in the technical data sheet.

All AlphaLISA assays were measured on the PerkinElmer EnSight multimode plate reader using default values for standard Alpha detection. Standard curves were prepared using recombinant human protein provided in each kit, in AlphaLISA Lysis Buffer for lysate samples and in the appropriate cell culture media for supernatant samples. Data were plotted in GraphPad Prism® and curves fit with nonlinear regression analysis using the four-parameter logistic equation (sigmoidal dose-response curve with variable slope) and  $1/Y^2$  data weighting. The lower detection limit (LDL) of the assay was calculated by taking three times the standard deviation of the average background values and interpolating from the standard curve. For biomarker assays, interpolated concentrations represent the amount of protein in the 5  $\mu$ L sample. For the AlphaLISA EGF/EGFR binding assay, inhibition curves were plotted and  $IC_{50}$  values were calculated according to a nonlinear regression using the 4-parameter logistic

equation sigmoidal dose-response curve with variable slope. All data shown is the average of a minimum of triplicate measurements (three microplate wells) unless otherwise specified.

## ATPlite 1step assays

Cellular health and proliferation were assessed by examining ATP content in cultures using ATPlite™ 1step (PerkinElmer, #6016731) following the standard protocol with a black BackSeal-96/384 applied prior to reading to eliminate cross-talk (PerkinElmer, #6005189; provided with ViewPlates). The resulting luminescence was measured using standard settings with the EnSight multimode plate reader.

## Results

### Cetuximab Blocks EGF Binding to EGFR

In addition to the detection of a desired target, AlphaLISA technology can be used to assess protein-protein binding and screen for inhibitors of binding. To demonstrate that cetuximab blocks the binding of the EGF ligand to EGFR, the AlphaLISA EGF/EGFR binding assay was used. In this assay, biotinylated EGF binds to Streptavidin-coated Donor beads, while EGFR-Fc is captured by anti-human IgG Fc-specific Acceptor beads (Figure 2A). Titrations of recombinant human EGF, cetuximab, and gefitinib were all examined for their ability to interfere with EGF binding to EGFR for which data are presented in Figure 2. As expected, recombinant EGF competes with the EGF in the kit to produce a concentration-dependent decrease in assay signal (Figure 2B). Cetuximab inhibits EGF binding to EGFR also in a concentration-dependent manner with  $IC_{50}$  values reported in Figure 2C. Gefitinib, however, is known to bind the intracellular portion of EGFR and does not inhibit EGF binding (Figure 2D).

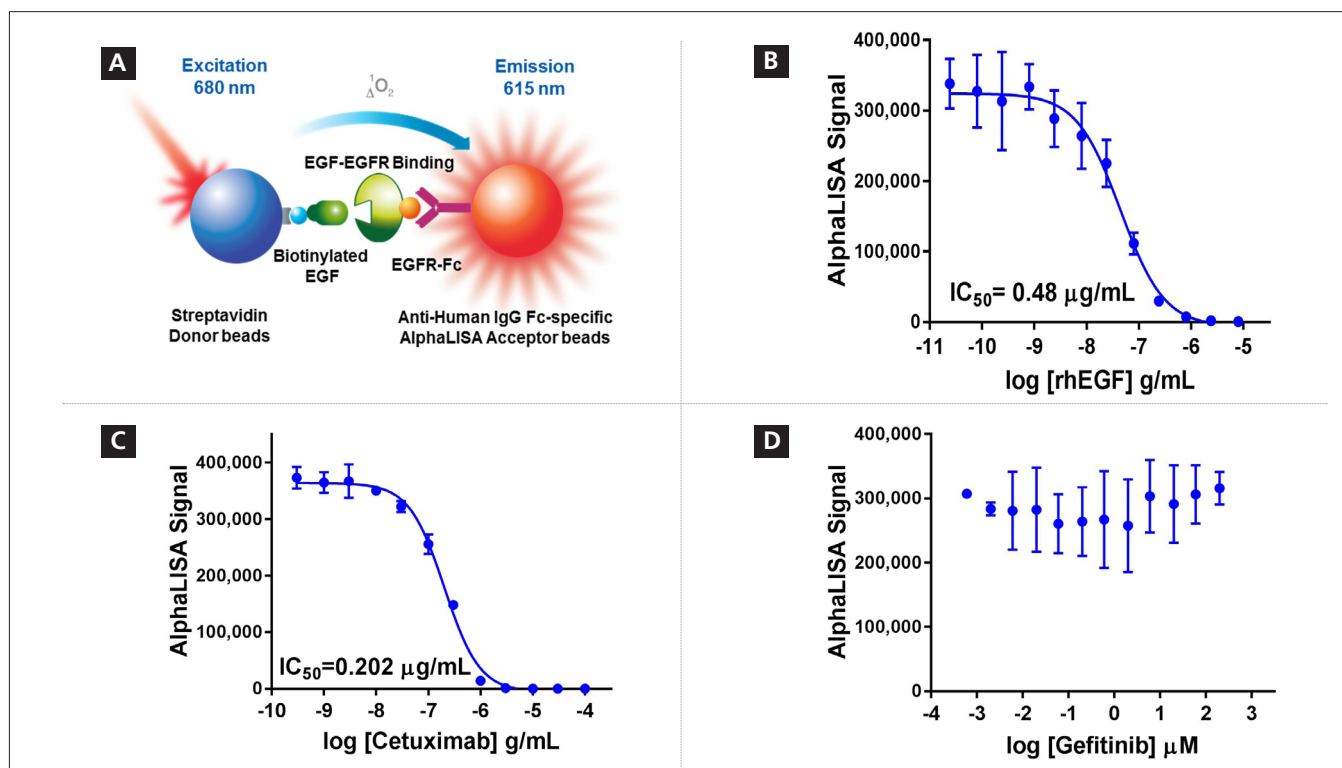


**Figure 2. Cetuximab inhibits EGF binding to EGFR measured using AlphaLISA.** A) Schematic of the AlphaLISA EGF/EGFR binding assay. B) Recombinant human EGF competes with biotinylated EGF binding. C) Cetuximab titration illustrates dose-dependent inhibition of EGF-EGFR binding. D) Gefitinib does not inhibit the binding interaction between EGF and EGFR (n=3 wells, error= SD).



## EGF Affects Both Cell Proliferation and Morphology in A431 Cells

In order to examine the effects of gefitinib and cetuximab, we chose two cell lines known to overexpress EGFR and tested the effects of exogenous treatment with EGF. A431 cells, derived from a female patient suffering from squamous cell carcinoma, and first have been used for many years to study EGFR structure, functions, and downstream signaling.<sup>6,11</sup> The A549 cell line is derived from human adenocarcinoma of the lung and is used as a model for non-small cell lung carcinoma (NSCLC).<sup>12</sup> According to a recent review, EGF concentrations can range widely in various organs of the human body, from below 1 ng/mL up to 500 ng/mL, so we assessed a wide range of concentrations in our cellular models.<sup>2</sup> To characterize the effects of EGF on cellular growth and proliferation, A431 and A549 cells were seeded at 10,000 and 5,000 cells per well, respectively, into separate 96-well plates. Cultures were incubated overnight to allow cells to attach and recover, then treated with varying concentrations of EGF. After two days, cell nuclei were labeled with Hoechst, imaged, and counted on the EnSight multimode plate reader.

Treatment with EGF has been shown to induce changes in A431 cell morphology and attachment,<sup>12,13</sup> which we observed in wells treated with higher concentrations of EGF. The images in Figure 3 illustrate the dramatic effects 10 ng/mL EGF had on A431 cellular morphology (Figure 3A), resulting in more sparse cultures

of narrow, spindle-shaped cells. There were no obvious effects observed on cellular morphology in A549 cultures (Figure 3B). To quantify the effects of EGF treatment on total cell number, the Kaleido software on the EnSight was used to automatically identify nuclei and count the total number of cells per well. In order to directly compare A431 and A549 cell proliferation, the number of cells per well in each treatment condition were normalized to the average number of cells per well in the untreated (no EGF) control wells and data presented in the same graph (Figure 3D). The data indicate that increasing concentrations of EGF result in a decrease in A431 cell numbers, consistent with a report that high concentrations of EGF can reduce proliferation and induce cell death pathways in A431 cells.<sup>14</sup>

Another method commonly used to assess levels of cellular health and proliferation is to measure the concentration of ATP. Using the ATPlite 1step assay, we observed that EGF treatment above 1 ng/mL resulted in increased concentrations of ATP in A549 cells (Figure 3E). Since there wasn't a concomitant increase in cell number, this increase in ATP suggests that EGF is acting to promote cellular health and growth in our cultures.<sup>15</sup> We also observed an increase in ATP in mid-range concentrations of EGF in A431 cultures, suggesting that these concentrations support cell growth, whereas higher concentrations do not. This is supported by a report that states picomolar concentrations of EGF can stimulate growth in A431 cells over longer periods of time (4-5 days).<sup>16</sup>

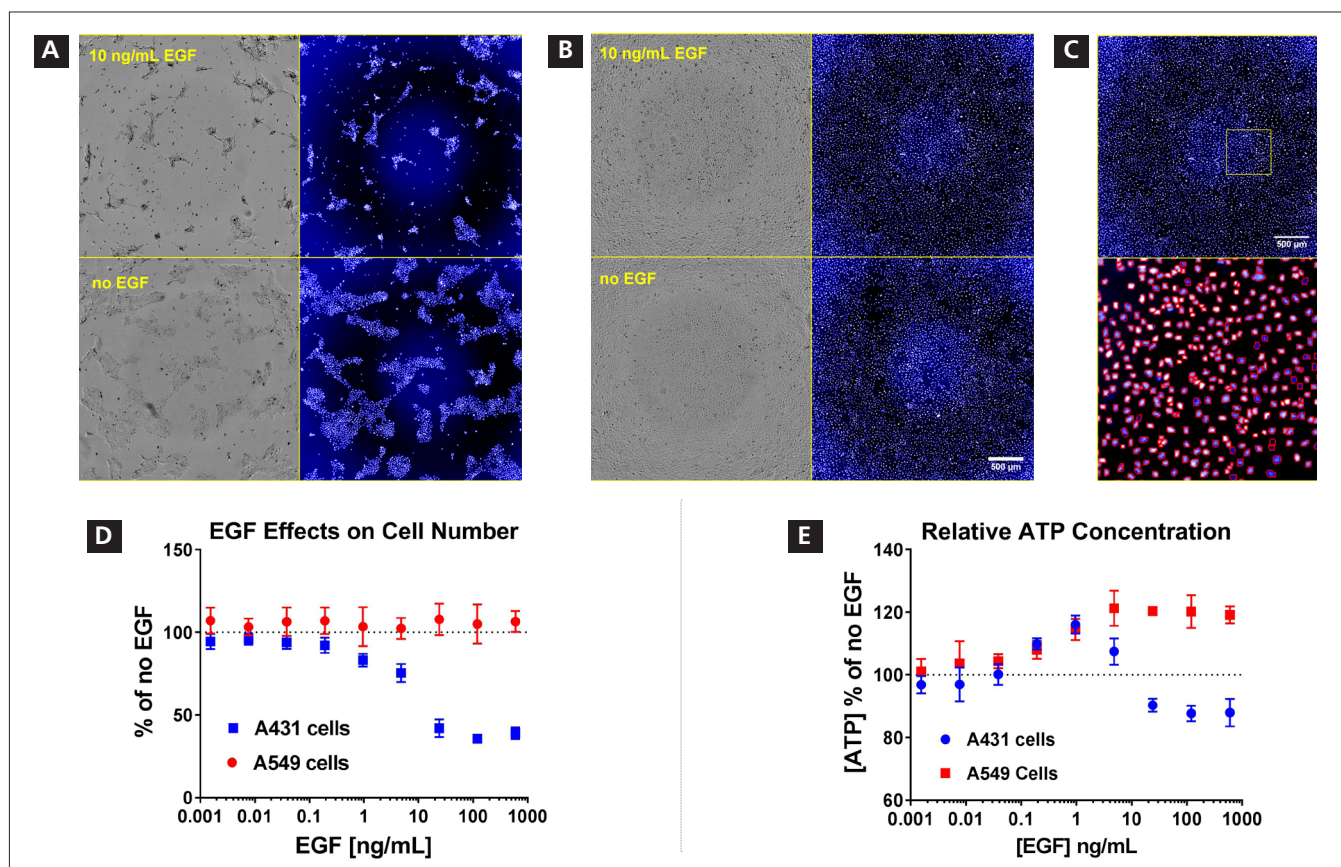


**Figure 3. EGF treatment effects on cellular morphology and the number of cells in culture.** Representative images of (A) A431 cells and (B) A549 cells treated for two days with 10 ng/mL EGF (top images) or no EGF (bottom) taken with the EnSight multimode plate reader using brightfield (grayscale images) and UV optics (blue images). (C) Individual nuclei were automatically identified and total number of cells per well calculated by the EnSight's Kaleido software as demonstrated by the red outlines in the bottom image, a zoomed in region from the image above (yellow box). (D) The number of cells per well in each condition normalized to the average number in wells with no EGF and graphed as a percent of no EGF. (E) The relative amount of ATP assessed with the ATPlite 1step assay and normalized as a percent of wells containing no EGF (n=3 wells, error=SD).

### Treatment with EGF Regulates EGFR Expression in A549 Cells

In order to assess the relative levels of EGFR present and the effects of sustained receptor stimulation with EGF for two days, cells were lysed after they were counted on the EnSight multimode plate reader. The lysates were assessed for EGFR concentration using the AlphaLISA EGFR detection assay following the assay workflow outlined in Figure 4A. The resulting concentrations of EGFR were interpolated from a standard curve (Figure 4B) produced by a titration of recombinant EGFR protein (provided in the kit). The average pg/mL of EGFR per well after treatment with different concentrations of EGF are presented in Figure 4C with concentrations for A431 cells in blue (left-side axis) and A549 in red (right-side axis). From this data, it appears that EGFR is expressed at about 10-fold higher concentrations in A431 cells compared to A549 cells. It also appears that treatment with increasing concentrations of EGF results in downregulation of EGFR expression levels in both cell lines. However, we have shown that EGF treatment affects cell numbers in A431 cells (Figure 3), and that could affect overall EGFR levels. In order to determine if the observed treatment effect on EGFR protein expression is a result of changes in cell number, EGFR protein levels were normalized to cell number by dividing the cell concentration by the number of cells counted in each well. The normalized values were then multiplied by a factor of 10,000 for graphing and data visualization purposes. The resulting normalized data (Figure 4D) showed that EGF treatment downregulates EGFR expression per cell in a dose-dependent manner in A549 cells but not in the A431 cells, illustrating the importance of counting and normalizing concentrations to cell number.

### Drug Treatment Effects on Cell Number

Since we established that concentrations above 1 ng/mL affect both cell lines by either reducing cell numbers in A431 cells or downregulating EGFR receptor expression in A549 cells, the next step was to examine drug treatment effects. For this, we first tested the effects of a two-day treatment with varying concentrations of each drug individually on cell numbers in each cell line without the addition of EGF. The data from these experiments indicate that treatment with gefitinib at concentrations above 1  $\mu$ M result in a significant decrease in cell number (Figure 5A) for both cell types. Cetuximab doesn't show much effect except to decrease A549 cell numbers at the highest concentration tested (100  $\mu$ g/mL). From these experiments, two concentrations of each drug that did not have effects alone on cell numbers were used to examine individual and combined effects of drug treatment on cell numbers and viability in cultures treated with 10 ng/mL EGF. The result of this cross-titration on cell numbers and ATP concentrations, shown in Figure 5C-F, are expressed as a percentage of the average result in control wells not treated with EGF or drug. The data indicate, for A431 cells, that cetuximab inhibits the EGF effect on cell number (Figure 5C) and ATP (Figure 5E), whereas gefitinib inhibits the effects on cell number but does not completely rescue the effect and appears to produce a growth inhibitory effect at these concentrations. For A549 cells, the drugs do not appear to have a strong effect on cell numbers (Figure 5D) but do inhibit the slight increase in ATP induced by EGF treatment (Figure 5F).

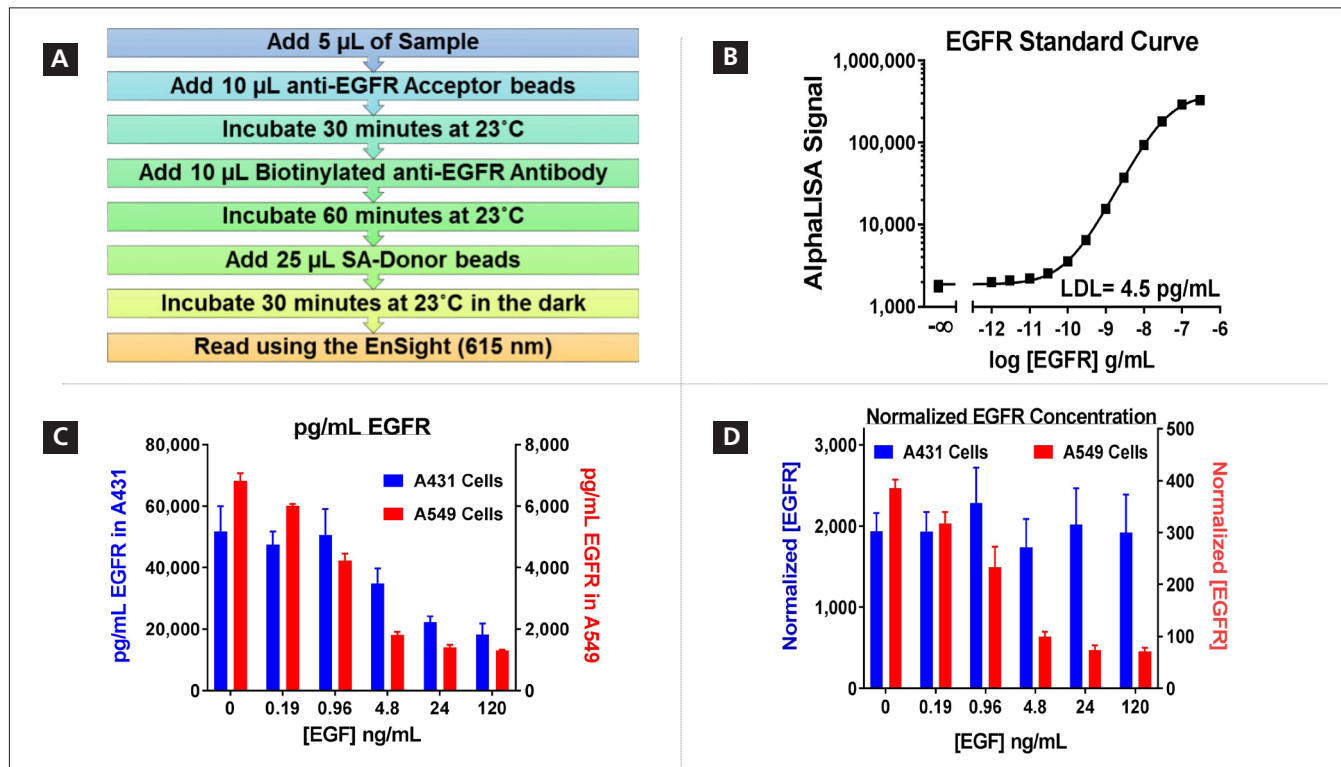


**Figure 4. EGFR Expression after two days of EGF treatment.** A) The AlphaLISA EGFR detection assay protocol. B) A standard curve generated from recombinant human EGFR protein concentrations and presented here to illustrate the sensitivity and dynamic range of the AlphaLISA assay. C) Concentrations of EGFR in pg/mL per well were interpolated from the standard curve and illustrate the effects of EGF treatment on A431 (left-side axis and blue bars) and A549 cells (right-side axis and red bars). D) EGFR protein concentrations normalized to cell number per well (and multiplied by a factor of 10,000) illustrate that EGF treatment induces a significant decrease in EGFR relative to cell number only in the A549 cultures.

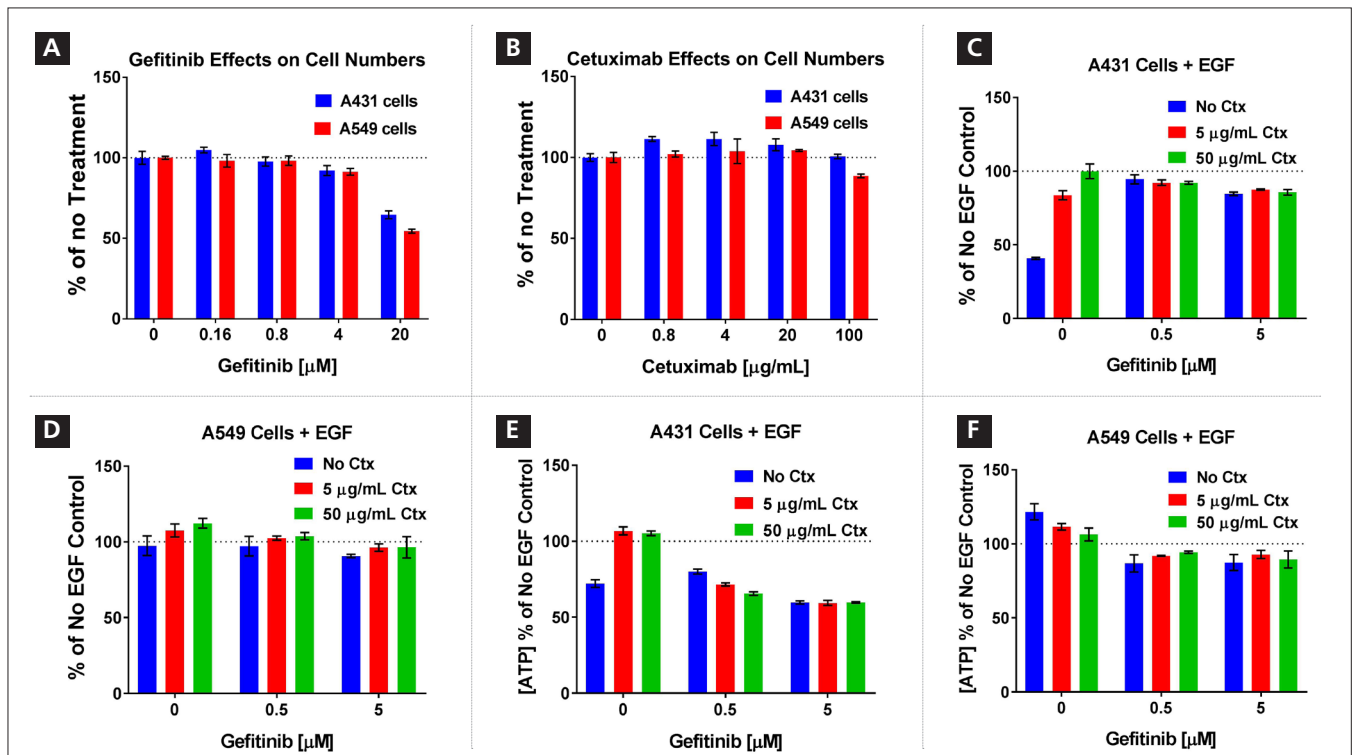


**Figure 5. Effects of drug treatment and inhibition of EGF-induced changes in cell numbers and ATP.** The effects of treatment for two days with varying concentrations of (A) gefitinib and (B) cetuximab (without added EGF) on the number of cells in culture presented normalized to wells receiving no treatment. To assess the ability of both drugs at inhibiting the effects of 10 ng/mL EGF two doses of gefitinib and cetuximab (Ctx) were used and effects on (C) A431 and (D) A549 cell counts were graphed relative to wells receiving no EGF and no drug. Effects were also assessed on relative ATP concentrations for (E) A431 and (F) A549 cells.

### Immune Checkpoint Proteins Regulated by EGFR Activation

With the need for developing combinatorial drug therapies to overcome resistance comes a requirement for discovering and characterizing more useful biomarkers that can predict therapeutic efficacy and resistance.<sup>9</sup> In addition to the expression of EGFR, other useful biomarkers for measuring cancer progression can include immune checkpoint proteins, secreted inflammatory cytokines, and chemokines. The upregulation of immune checkpoint proteins, such as PD-L1, permit tumor cells to escape targeting by the immune system so factors that regulate the expression of these proteins can affect cancer progression and resistance to different drug classes. Many recent reports are available linking PD-L1 expression to the EGFR pathway<sup>17,18</sup> including a recent report describing the development of a bispecific antibody that targets both PD-L1 and EGFR.<sup>19</sup> CD276 (B7-H3) is another important immune checkpoint protein that is overexpressed in a wide range of cancers and correlates with negative prognosis and poor clinical outcome in patients, but much less is known about its receptors and activities.<sup>20</sup>

In order to assess the levels of PD-L1 and CD276 in these cell models and the effects of EGF treatment and EGFR-targeted therapies on expression levels, AlphaLISA detection assays were run on lysate samples from the same wells that were counted and assessed for EGFR protein expression levels. Relative concentrations of each protein were normalized to cell number and then divided by the average normalized concentration from wells receiving no treatment (no drug and no EGF). The data from these experiments indicate that EGF treatment induces a dose-dependent upregulation of PD-L1 (Figure 6A) in both cell types. The increase in PD-L1 caused by EGF treatment is inhibited by both cetuximab and gefitinib and the effect of both appears to be additive (Figure 6B-C), causing a

reduction in PD-L1 expression levels below the untreated EGF control and supporting a link between EGFR signaling and PD-L1 expression. This suggests that any endogenous signaling occurring through the EGFR pathway is impacted by drug treatment and this further regulates PD-L1 expression levels.

For CD276 expression, the effects of treatment differ by cell type (Figure 6D-F). CD276 protein expression appears to be upregulated by EGF treatment in A431 cells but not A549 cells (Figure 6D). The upregulation of CD276 by EGF observed in A431 cells is blocked by treatment with gefitinib and expression levels are further inhibited by treatment with the higher concentration of cetuximab (Figure 6E). Though A549 cells do not show EGF-induced upregulation of CD276, there may be an effect of higher concentrations of cetuximab on reducing levels of CD276 (Figure 6F).

### Chemokines Affected by EGF Titration Can Be Inhibited by Drug Treatment

Secretion of chemokines and cell surface expression of their receptors are upregulated in many cancers and facilitate tumor growth.<sup>21</sup> GRO (Growth regulated oncogene)- $\alpha$  (also known as CXCL1) is a chemotactic cytokine known to regulate cancer progression and invasion. Interleukin-8 (IL-8, or CXCL8) is a proinflammatory chemokine that can be regulated by a variety of stimuli, including inflammatory signals and chemical stresses like exposure to chemotherapeutic drugs. Both GRO- $\alpha$  and IL-8 have been reported to be overexpressed in A431 cells.<sup>22</sup> We observe an upregulation of both GRO- $\alpha$  and IL-8 with EGF treatment in both cell types (Figure 7A, D). In addition, the increased secretion induced by treatment with 10 ng/mL of EGF is blocked by treatment with cetuximab and gefitinib for GRO- $\alpha$  (Figure 7B, C) and IL-8 (Figure 7E, F) in both cell lines.



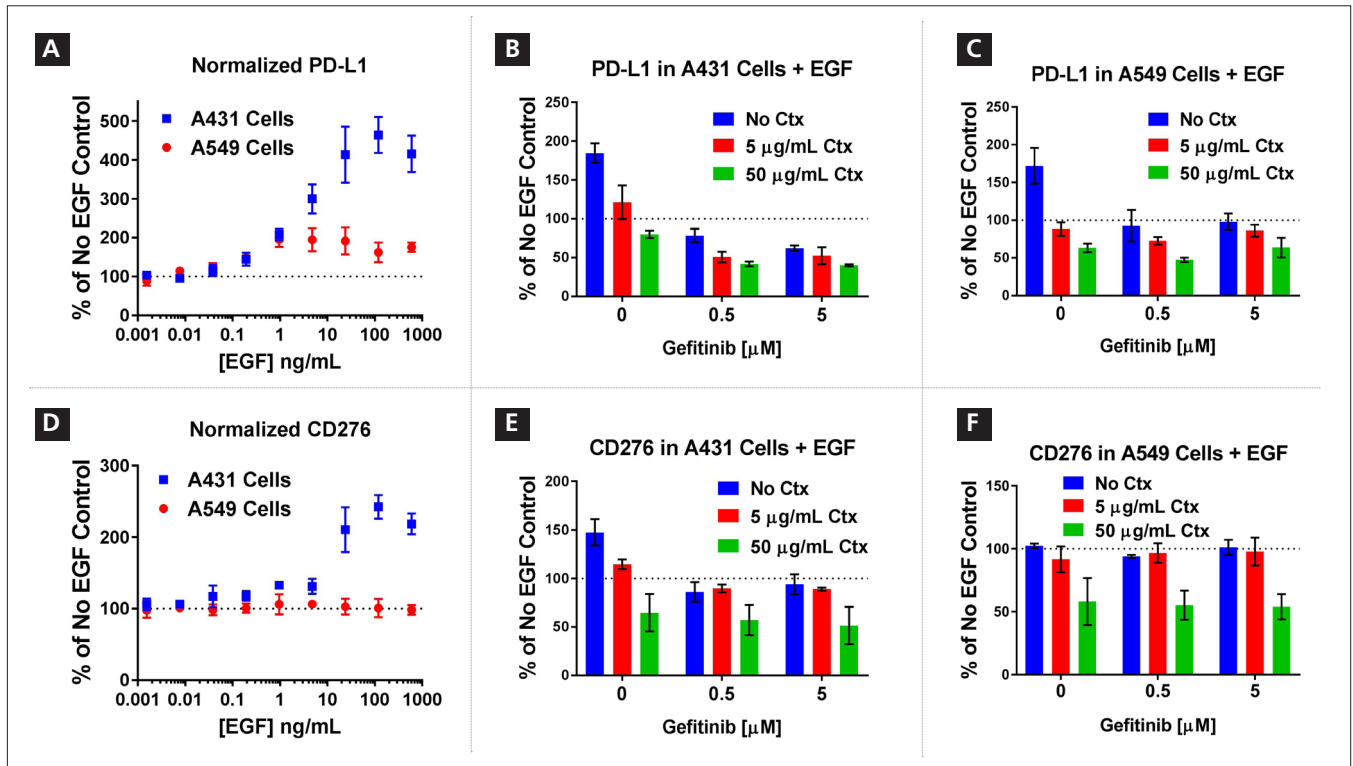


**Figure 6. Drug treatment effects on EGF-induced increases in the expression of immune checkpoint proteins PD-L1 and CD276.** The effects of treatment with EGF on the expression of (A) PD-L1 and (D) CD276 expressed as a percentage of no EGF control wells illustrate the differences in biomarker expression in A431 and A549 cells. Cross-titration effects of gefitinib and cetuximab (Ctx) treatment on PD-L1 expression in (B) A431 and (C) A549 cells treated with 10 ng/mL EGF. Drug effects on the EGF-induced changes in expression of CD276 were also examined for (E) A431 and (F) A549 cells. All data were first normalized to cell number per well and then expressed as a percentage of control wells only receiving fresh media (no EGF and no drug).

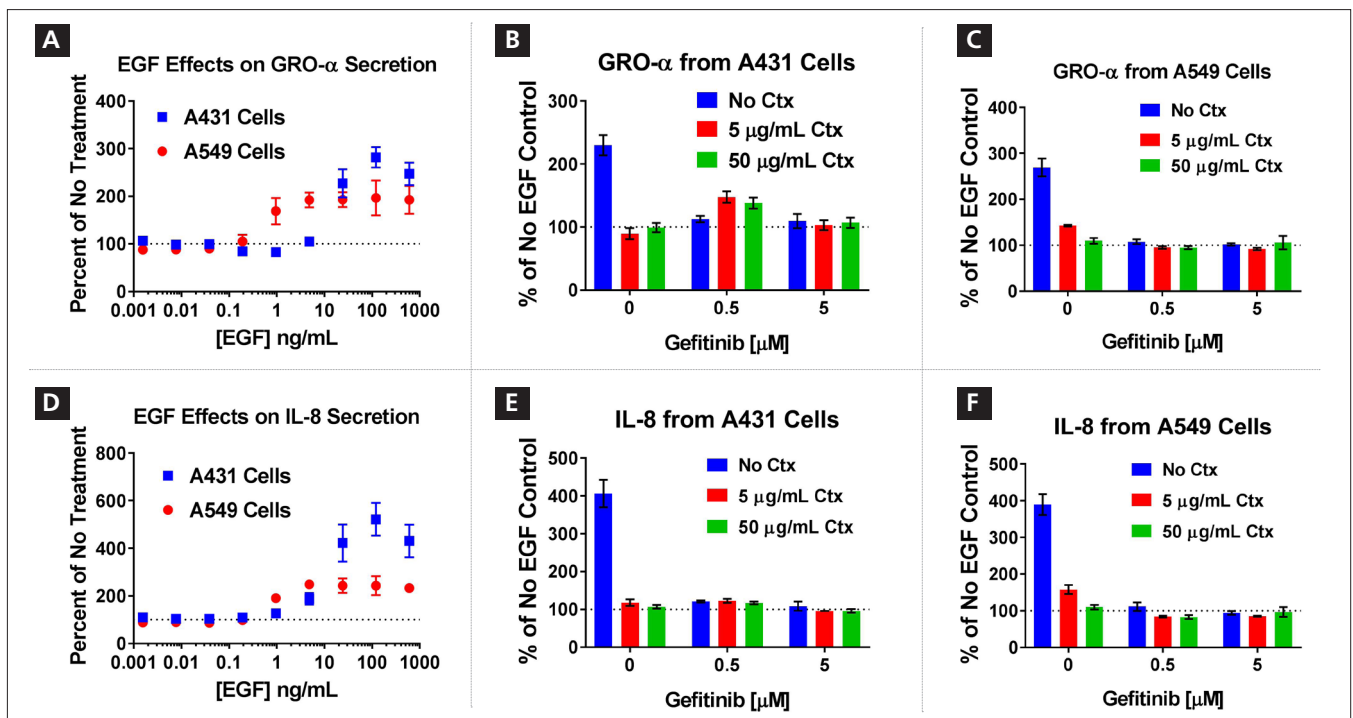


**Figure 7. Effects on secretion of chemokines IL-8 and GRO- $\alpha$ .** The effects of treatment with EGF on the secretion of (A) GRO- $\alpha$  and (D) IL-8 in both A431 and A549 cultures relative to control wells not treated with EGF. Effects of gefitinib and cetuximab (Ctx) treatment on secretion of GRO- $\alpha$  and IL-8 in A431 (B, E) and A549 (C, F) cells treated with 10 ng/mL EGF. All data were normalized to cell number per well and then expressed as a percentage of control wells (no EGF and no drug).

## Effects on Secretion of Angiogenesis promoting factors

Angiogenic growth factors are another class of biomarkers that have been examined in patient samples as a means of measuring treatment efficacy.<sup>23</sup> One soluble factor highly expressed by a variety of cancers is vascular endothelial growth factor (VEGF), a known mediator of angiogenesis and promoter of tumor progression. Disruption of EGFR activation has been reported to affect VEGF levels in culture.<sup>24</sup> We examined the effects of treatment on relative VEGF concentrations in our cell cultures and found that, once normalized to cell numbers, there was a clear increase in VEGF secretion induced by EGF treatment in A431 but not in A549 cells (Figure 8A). The effect of EGF treatment on VEGF secretion was inhibited by both cetuximab and gefitinib (Figure 8B).

Tissue inhibitors of metalloproteinases (TIMPs) are a family of protease inhibitors that inhibit matrix metalloproteinases (MMPs), blocking proteolytic activity and minimizing extracellular matrix degradation, therefore promoting angiogenesis and cellular proliferation. Much like VEGF, the effects of EGF on TIMP-2 secretion is only observed in the A431 cell line. However, the increase in TIMP-2 expression in A431 cells only appears to be inhibited by cetuximab, whereas treatment with gefitinib shows no effect (Figure 8E). This effect was also observed in a separate experiment with just gefitinib treatment alone producing increased TIMP-2 secretion in A431 cellular supernatants at concentrations as low as 160 nM gefitinib (data not shown). EGF treatment has been shown to upregulate TIMP-2 expression in four neural progenitor cell lines<sup>25</sup> whereas treatment with exogenous TIMP-2 has been shown to inhibit EGFR phosphorylation and EGF-induced proliferation in A549 cells.<sup>26</sup>

This suggests that TIMP-2 and EGFR signaling can interact in very different ways in different cell types, which is what we observed here with our two cell lines.

## Conclusion

Since resistance mechanisms often develop to individual drug therapies, more combinatorial studies are being performed to seek additional modes of treatment for cancers where EGFR is overexpressed. In addition, the data presented here indicate that treatment with different EGFR-targeted therapies can result in varied responses in cell proliferation, viability, and the expression of key biomarkers in different cancer-derived cell lines that overexpress EGFR. This indicates a need for more research into categorizing the combined effects of different therapies and a more comprehensive assessment of multiple cellular outputs affected by these treatments.<sup>9,27</sup>

Here, we demonstrated a method to rapidly measure the effects of two EGFR-targeted drugs with different modes of action on cellular growth and the expression of key biomarkers using the EnSight multimode plate reader with imaging capabilities and multiple AlphaLISA detection assays on samples from the same wells of a culture plate. The vast array of AlphaLISA detection assays allow for multiple key cancer markers to be analyzed quickly using small samples from the same well. Most AlphaLISA assay workflows consist of only a few simple addition steps and require at most 5  $\mu$ L of sample per target. AlphaLISA assays can be read on all Alpha-enabled plate readers such as PerkinElmer's EnSight and EnVision® multimode plate readers and can be easily automated for screening with liquid handling automation platforms like PerkinElmer's JANUS® Automated Workstation to enhance productivity.

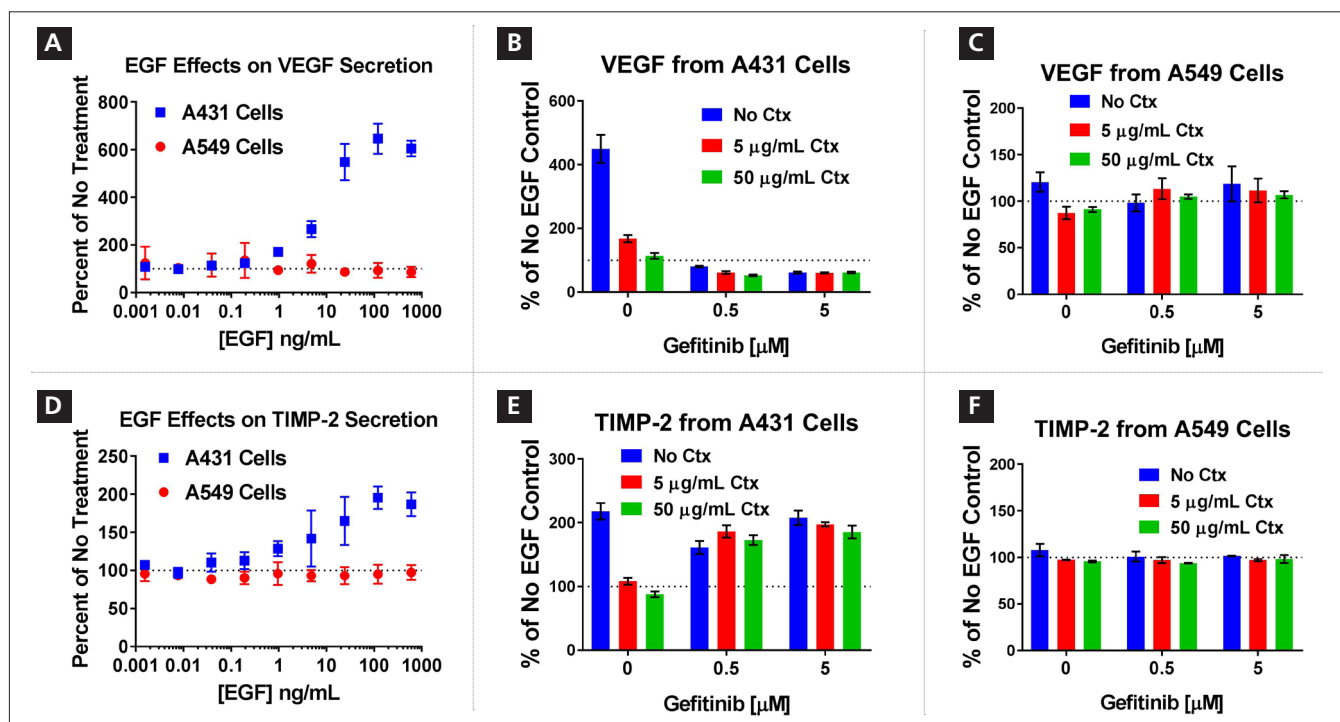


**Figure 8. Treatment effects on expression of angiogenesis markers.** A) EGF treatment increased VEGF secretion in A431 cells but not A549 cells and this increase was blocked by both cetuximab and gefitinib (B). D) TIMP-2 concentration in supernatants increased with EGF treatment in A431 cultures and this was inhibited by cetuximab and not gefitinib (E). In A549 cells, VEGF (C) and TIMP-2 (F) levels were not significantly affected by drug or EGF treatment.



## References

- Chen, J., (2016). Expression and function of the epidermal growth factor receptor in physiology and disease. *Physiol Rev*, 96: 1025-69.
- Wee, P.& Wang, Z. (2017). Epidermal Growth Factor receptor cell proliferation and signaling pathways. *Cancers (Basel)*, 9(5): 52-96.
- Sigismund, S., et al. (2018). Emerging functions of the EGFR in cancer. *Molecular Oncology*, 12(1): 3-20.
- Thomas, R. and Weihua, Z. (2019). Rethink of EGFR in cancer with its kinase independent function on board. *Frontiers in Oncology*, 9(800): 1-16.
- Matar, P. (2004). Combined epidermal growth factor receptor targeting with the tyrosine kinase inhibitor gefitinib (CD1839) and the monoclonal antibody cetuximab (IMC-C225): Superiority over single-agent receptor targeting. *Clinical Cancer Research*, 10: 6487-6501.
- Brand, T. et al. (2011). Molecular Mechanisms of resistance to the EGFR monoclonal antibody cetuximab. *Cancer Bio. Ther.*, 11(9): 777-792.
- Tong, C.W.S. et al. (2017). Drug combination approach to overcome resistance to EGFR tyrosine kinase inhibitors in lung cancer. *Cancer Letters*, 405: 100-110.
- Baselga, J. (2001). The EGFR as a target for anticancer therapy — focus on cetuximab. *Eur. J. Cancer* 37: S16–S22.
- Patil, N. et al. (2012). Cetuximab and biomarkers in non-small-cell-lung carcinoma. *Biologics: Targets and Therapy*, 6: 221-231.
- Segovia-Mendoza, M. (2015). Efficacy and mechanism of action of the tyrosine kinase inhibitors gefitinib, lapatinib, and neratinib on the treatment of HER2-positive breast cancer: preclinical and clinical evidence. *Am J Cancer Res*, 5(9): 2531-61.
- Rexer, B.N., et al. (2009). Overcoming resistance to tyrosine kinase inhibitors: Lessons learned from cancer cells treated with EGFR antagonists. *Cell Cycle*, 8(1): 18-22.
- Tong, A.W. (2006). Small RNAs and non-small cell lung cancer. *Curr Mol Med*, 6(3): 339-49.
- Lu, Z., et al. (2001). Epidermal growth factor-induced tumor cell invasion and metastasis initiated by dephosphorylation and downregulation of focal adhesion kinase. *Molecular and Cellular Biology*, 21(12): 4016-31.
- Kim, K., et al. (2015). Epidermal growth factor-induced cell death and radiosensitization in epidermal growth factor receptor-overexpressing cancer cell lines. *Anticancer Research*, 35: 245-254.
- Chan, G.K., et al. (2013). A simple high-content cell cycle assay reveals frequent discrepancies between cell number and ATP and MTS proliferation assays. *PLoS One*, 8(5): e63583.
- Kawamoto, T., et al. (1983). Growth stimulation of A431 cells by epidermal growth factor: Identification of high-affinity receptors for epidermal growth factor by anti-receptor monoclonal antibody, *Proc Natl Acad Sci*, 80: 1337-1341.
- Okita, R., et al. (2017). PD-L1 overexpression is partially regulated by EGFR/HER2 signaling and is associated with poor prognosis in patients with non-small-cell lung cancer. *Cancer Immunol Immunother*, 66(7): 865-876.
- Ritprajak, P. & Azuma, M. (2015). Intrinsic and extrinsic control of expression of the immunoregulatory molecule PD-L1 in epithelial cells and squamous cell carcinoma. *Oral Oncol*, 51(3): 221-8.
- Koopmans, I., et al. (2018). A novel bispecific antibody for EGFR-directed blockaded of the PD-1/PD-L1 immune checkpoint. *Oncoimmunology*, 7(8):e1466016.
- Picarda, E., et al. (2016). Molecular Pathways: Targeting B7-H3 (CD276) for human cancer immunotherapy, *Clin Cancer Res*, 22(14): 3425-3431.
- Raman, D., et al. (2007). Role of chemokines in tumor growth. *Cancer Letters*, 256(2): 137-165.
- Metzner, B., et al. (1999). Overexpression of CXC-chemokines and CXC-chemokine receptor type II constitute an autocrine growth mechanism in the epidermoid carcinoma cells KB and A431. *Oncology Reports*, 6(6): 1405-10.
- Lawicki, S., et al. (2017). Plasma levels and diagnostic utility of VEGF, MMP-2, and TIMP-2 in the diagnostics of breast cancer patients. *Biomarkers*, 22(2): 157-164.
- Petit, A.M., et al. (1997). Neutralizing antibodies against epidermal growth factor and ErbB-2/neu receptor tyrosine kinases down-regulate vascular endothelial growth factor production by tumor cells in vitro and in vivo: angiogenic implications for signal transduction therapy of solid tumors. *Am J Pathol*, 151(6): 1523-30.
- Jaworski, D.M. & Perez-Martinez, L. (2006). Tissue inhibitor of metalloproteinase-2 (TIMP-2) expression is regulated by multiple neural differentiation signals. *J Neurochem*, 98(1): 234-247.
- Hoegy, S.E., et al. (2001). Tissue inhibitor of metalloproteinases-2 (TIMP-2) suppresses TKR-growth factor signaling independent of metalloproteinase inhibition. *The Journal of Biological Chemistry*, 276(5): 3203-3214.
- Marmaerlis, M.E. & Aggarwal, C. (2018). Combination immunotherapy in non-small cell lung cancer, *Current Oncology Reports*, 20(7): 55.